Comparative Design and Performance Analysis of Multiband MIMO Antenna for Sub-6 GHz 5G Network

.

ABSTRACT

This paper presents the design and performance comparison of a multiband dual diversity 8-element multiple-input multiple-output (MIMO) antenna with a 4-element MIMO antenna with defected ground structure (DGS) at 2.45/3.5/5.2/6 GHz. The proposed antennas were designed on a flame retardant (FR-4) having a dielectric constant of 4.4 ($\varepsilon_r = 4.4$), dimensions of $200 \times 200 \times 1.6\,mm$ and $140 \times 90 \times 1.6\,mm$, respectively. The antennas were simulated and analyzed using Computer Simulation Studio (CST Studio). Results obtained from the simulation showed that the 8-element MIMO antenna achieved a combined bandwidth of 908.68 MHz. In contrast, the 4-element MIMO antenna with DGS achieved 4.22 GHz bandwidth on average. Broadside radiation pattern was observed across the three frequency bands in both E- and H-plane with an average main lobe magnitude of 7.8 dBi. Furthermore, the proposed antennas achieved consistent Envelop Correlation Coefficient (ECC) and Diversity Gain (DG) values of 0.0008 and 9.999 and Port-to-port isolation of 27 dB across all frequencies considered. Also, an antenna gain of 8.58 dB was achieved at a frequency of 6 GHz for the 8-element MIMO antenna, while a maximum gain of 5.58 dBi was achieved by the 4-element MIMO antenna with DGS. The gain, isolation, DG, and ECC between adjacent ports and the loss in capacity were within the standard margins, making the antenna structure suitable for MIMO applications.

Keywords: Multiband, MIMO antenna, defected ground structure (DGS), sub-6 GHz 5G, comparison

1. INTRODUCTION

Release 8 from Third Generation Partnership Progress (3GPP) saw the introduction of Multiple-Input Multiple-Output (MIMO) technology along with Long Term Evolution (LTE) Standard [1]. According to [2], MIMO technology is defined as a wireless technology that increases the data capacity of a Radio Frequency (RF) channel by using multiple transmitting and receiving antennas. The increased capacity is achieved by taking advantage of multiplexing gain and diversity. Two broad categories of MIMO technology generally known are Single User MIMO (SU-MIMO) and Multi-User MIMO (MU-MIMO) [2]. The former refers to the adoption of multiple transmitting antennas and a receiver for communication, while the latter is the adoption of multiple antennas at either end of the communication link. The adoption of MIMO technique in wireless communication was borne out of the desire to overcome the complications associated with a single antenna transmission system. The LTE communication standard takes advantage of characteristics such as beamforming gain, spatial/polarization diversity, and spatial multiplexing [3]. Chattha [4], in his submission, stated that MIMO technology uses multipath to achieve higher data rates, thereby simultaneously increasing reliability and range without using extra bandwidth, thus improving spectral efficiency to cope with the need for high data rates for different services. The author added that antenna diversity is one of the prominent techniques used in cubbing multipath fading in no clear line-of-sight (LoS) radio channel in that it implements either spatial, pattern, polarization diversity, or a combination of these. By

interpretation, Jamshed et al. [5] highlighted that to fully explore diversity gain for 5G communication, more than one diversity scheme implementation is recommended and this is only achievable with a multi-element antenna configuration.
This paper compares the performance of two MIMO antennas: an 8-element MIMO antenna and a single-element multifrequency MIMO antenna with a defected ground structure (DGS). Both antennas were designed on a flame retardant (FR-4) substrate for multifrequency applications, including C-band 5G deployment frequency for the Nigerian market and frequency bands for Wireless Fidelity (WiFi) and WiFi 6 standards as put forward by the Institute of Electrical Electronics Engineering (IEEE).

2. REVIEW OF RELATED LITERATURE

Several authors have explored microstrip patches as a viable option in deploying MIMO technology. Shoaib *et al.*[6] presented the design of MIMO antennas for mobile handsets covering the GSM 1800/1900 band, Wireless Local Area Network (WLAN), and some LTE bands. Nithya *et al.*[7] proposed an eight-element MIMO antenna for 5G smartphones, which resonated at 3.8, 4.5 and 5.8 GHz. Lee et al. [8] presented a close-mounted mobile handset MIMO antenna for LTE 13 band application.Abdulkareem and Farhan [9] and Singh *et al.* [10] put forward their designsof novel MIMO antenna geometry for both sub-6 GHz and mm-Wave 5G communication with viable submissions.Though these publications met their different outlined objectives, they did not optimize for the frequency range considered in this study.

Multiband MIMO antenna with defective ground structure was presented by Sarade and Ruikar[11] for review. Suggestions were made regarding general design approach to microstrip antenna. No antenna was presented for comparison.

Al-Ajrawi and Rahhal [12] presented the design of a 2×33 mMIMO antenna using an inset-fed rectangular microstrip antenna as the primary element at 1.5 GHz on a Rogers Ultralam 1217 (tm) substrate material. The antenna was reported to have better antenna characteristics than the single-band antennas. However, despite the number of elements constituting their mMIMO antenna, the realised gain was not significantly improved over the single-band antenna gain.

A design to boost mMIMO antenna performance and improve isolation between antenna elements was presented by Sandi et al. [13] in their article. They used a 5G frequency spectrum of 3.5 GHz with dielectric resonators, electromagnetic bandgap (EBG), and defected ground structure (DGS) approaches. FR-4, a substrate material with a dielectric constant (εr) of 4.3, was utilised. Simulation and test results demonstrated enhanced mutual coupling, expanded bandwidth, and higher antenna gain. Their suggested antenna covers a different frequency range than what is shown in this study.

The design and analysis of a 72 port (288 antennas) triangular-shaped mMIMO antenna system for 5G base stations was presented by Al-Tarifi et al. [14]. Their suggested antenna system consisted of three (3) layers on each side, with a total of 24 ports and a footprint of $44.4 \times 29.6 \times 0.1524\, cm^3$. Every port (subarray) was comprised of 2×2 patches on the upper layer, a pre-calculated feed network on the lower layer, and a ground plane forming the intermediate layer. Their suggested antenna's resonance was achieved in two different operating modes. For high signal-to-noise-ratio (SNR) circumstances, the initial mode was an individual MIMO mode with little correlation across distinct ports (each subarray operated independently and had beams directed away from its adjacent elements). In the second mode, customers have dedicated beams thanks to array beam switching for instances with

UNDER PEER REVIEW

lower SNR. Their low bandwidth prevented it from achieving large antenna gain despite its presentation (100 MHz).

3. METHODOLOGY

The design of the constituent single-band microstrip antennas follows the transmission line equations for designing rectangular antennas from [15]. The basic parameters of the microstrip, such as the width, length, and dimensions of the microstrip line, are determined as follows:
The width of the patch W_p is determined from Equation 1:

$$W_p = \frac{c}{2f_r}\sqrt{\frac{2}{\varepsilon_r+1}} \quad (1)$$

where c, f_r and ε_r are the speed of light, design frequency and relative permittivity.

The patch length is calculated using Equation 4, however, the length's extension, ΔL and the effective permittivity, ε_{reff} are first calculated from Equations 2 and 3 before the length of the microstrip patch. The substrate thickness, h of 1.6 mm, is maintained throughout the design. The effective dielectric constant and length extension are calculated thus:

$$\varepsilon_{reff} = \frac{\varepsilon_r+1}{2} + \frac{\varepsilon_r-1}{2}\left[1+12\frac{h}{W_p}\right]^{-\frac{1}{2}} \quad (2)$$

$$\Delta L = 0.412h\ \frac{(\varepsilon_{reff}+0.3)\left[\frac{W_p}{h}+0.264\right]}{(\varepsilon_{reff}-0.258)\left[\frac{W_p}{h}+0.8\right]} \quad (3)$$

The patch length is calculated from Equation 4 thus:

$$L = \frac{c}{2f_r\sqrt{\varepsilon_{reff}}} - 2\Delta L \quad (4)$$

As earlier stated, inset feeding technique was used to offset the feeding location to the point where an impedance match between the patch and feedline can be achieved. The inset feed parameters are determined using the following equations.
To calculate the notch width, g equation from [12] is employed as given in Equation 5.

$$g = \frac{c\, f_r \times 10^{-9} \times 4.65 \times 10^{-9}}{\sqrt{2\varepsilon_{reff}}} \quad (5)$$

The resonant input resistance R_{in} is calculated from Equation 6;

$$R_{in}(y=y_o) = \frac{1}{2(G_1+G_{12})}\cos^2\left(\frac{\pi y_o}{L_p}\right) \quad (6)$$

The equation for the characteristic impedance Z_o is given in Equation 7;

$$Z_0 = \begin{cases} \frac{60}{\sqrt{\varepsilon_{reff}}}\ln\left[\frac{8h}{W_f}+\frac{W_f}{4h}\right] & \text{for } \frac{W_f}{h} \le 1 \\ \frac{120\pi}{\sqrt{\varepsilon_{reff}}}\left[\frac{W_f}{h}+1.393+0.667\ln\left(\frac{W_f}{h}+1.444\right)\right] & \text{for } \frac{W_f}{h} \ge 1 \end{cases} \quad (7)$$

In this design, the ratio, $\frac{W_f}{h} = \frac{2.98}{1.6} = 1.863 > 1$, so the second expression in Equation 7 applies.
Edge impedance, $R_{in(edge)}$ is computed from Equation 8.

$$R_{in(edge)} = \frac{1}{2(G_1 \mp G_{12})} \quad (8)$$

As reported by [15], the plus (+) sign is used for modes with odd (antisymmetric) resonance voltage distribution beneath the patch and between the slots, while the minus (-) sign is used for modes with even symmetric resonant voltage distribution. Other parameters such as wave number k, input current I1, input conductance G1, and mutual conductance G12 must first be known to evaluate the input resistance. The equations for computing the various parameters highlighted are given in Equations 9 to 13.

$$k = \frac{2\pi}{\lambda_{air}} \quad (9)$$

$$I_1 = -2 + \cos(X) + XS_i(X) + \frac{\sin(X)}{X} \quad (10)$$

UNDER PEER REVIEW

$$X = kW_p \quad (11)$$

$$G_1 = \frac{I_1}{120\pi^2} \quad (12)$$

$$G_{12} = \frac{1}{120\pi^2}\int_0^{\pi}\left[\frac{\sin(\frac{kW_p}{2}\cos\theta)}{\cos\theta}\right]^2 J_o(kL_p\sin\theta)\sin^3\theta d\theta \quad -(13)$$

where J_o is the Bessel function of the first kind of order zero. G_{12} is resolved using MATLAB script to calculate rectangular microstrip antenna parameters in conjunction with equations from [16].

Inset feed technique is used with a chosen characteristic impedance of 50 Ω; the design procedure is illustrated in [17].

The length of the ground plane (L_g) is:

$$L_g = 6h + L_p \quad (14)$$

The width of the ground plane is:

$$W_g = 6h + W_p \quad (15)$$

The geometry of the designed single-band RMSAs is depicted in the schematic diagram presented in Figure 1, while the computed values are presented in Table 1.

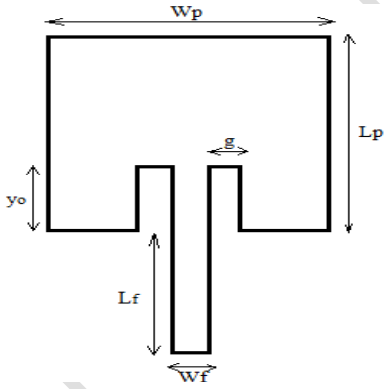

Fig. 1.Geometry of the designed antenna

In combining multiple elements on a single substrate, the challenge of mutual coupling of antenna elements arises due to the simultaneous reflections at similar frequencies [18]. However, as stated by [19], to lower the risk of mutual coupling, maintain single-mode propagation among radiating elements, and have in-phase element characteristics as well as radiation in the normal direction, the distance between elements is approximated to be about half wavelength $\left(\frac{\lambda_{air}}{2}\right)$; thus,

patch spacing (d) $= \frac{\lambda_{air}}{2}$

$$= \frac{85.71}{2} = 42.90\ mm.$$

Another notable reason a good separation distance, d, is necessary is that it enhances the ability to introduce space diversity within the antenna-integrated device. Saurabh *et al.*[20] proposed the orthogonal placement of antenna elements to achieve high isolation, especially with an interconnected ground plane from which the antenna elements are placed on the proposed MIMO antenna layout. Hence, a pair of each adjourning single-band antenna element will be placed orthogonally for the proposed design. With this approach, polarization diversity (linear and circular polarization) is easily achieved, as depicted in Figures 3 and 4. The substrate dimensions are $120 \times 120 \times 1.6\ mm$ for the 4-element MIMO antenna and $200 \times 200 \times 1.6\ mm$ for the 8-element MIMO antenna.

UNDER PEER REVIEW

Four rectangular single-band antennas designed at 2.45 GHz, 3.5 GHz, 5.2 GHz, and 6 GHz in CST Microwave Studio are presented in Figure 2, while 4-element antenna and 8-element MIMO antenna are presented in Figures 3 and 4, respectively.

Table 1.Design dimensions of single band inset-fed RMSAs

Design Parameter	2.45 GHz	3.5 GHz	5.2 GHz	6 GHz
Length (L_p)	28.83 mm	20.22 mm	13.20 mm	11.33 mm
Width (W_p)	37.26 mm	26.08 mm	17.56 mm	15.21 mm
Dielectric constant (ε_r)	4.4	4.4	4.4	4.4
Substrate height (h)	1.60 mm	1.60 mm	1.60 mm	1.60 mm
Patch thickness (t)	0.035 mm	0.035 mm	0.035 mm	0.035 mm
Length of ground plane (L_g)	38.43 mm	29.82 mm	22.80 mm	20.93 mm
Width of ground plane (W_g)	46.86 mm	35.68 mm	27.16 mm	24.81 mm
Width of inset feed (W_f)	3.10 mm	3.10 mm	3.06 mm	3.02 mm
Inset distance (y_0)	10.69mm	7.41 mm	4.89 mm	3.76 mm
Inset gap (g)	1.20 mm	1.73 mm	1.53 mm	1.56 mm
Length of 50 Ω transmission line (L_f)	4.80 mm	4.80 mm	4.80 mm	4.80 mm
Input edge impedance of the patch (R_{in})	320.11 Ω	320.11 Ω	317.60 Ω	316.33 Ω
Characteristic impedance of the feed line (Z_0)	50 Ω	50 Ω	50 Ω	50 Ω

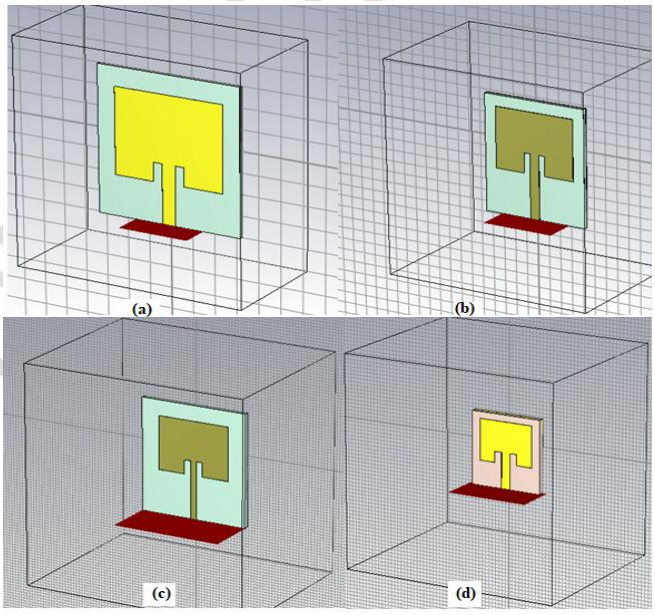

Fig. 2. Designed single band antenna (a) at 2.45 GHz (b) at 3.5 GHz (c) at 5.2 GHz (d) at 6 GHz

UNDER PEER REVIEW

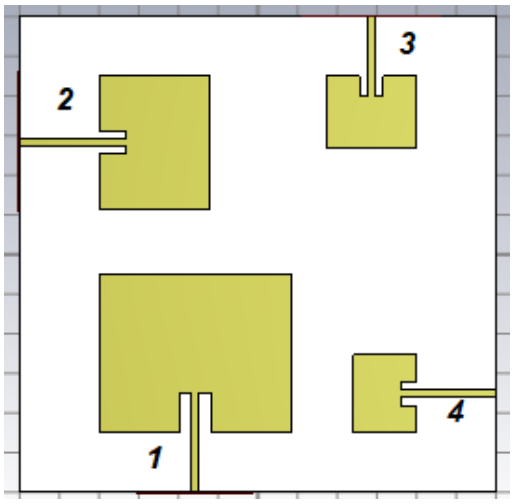

Fig. 3. Designed 4-element antenna

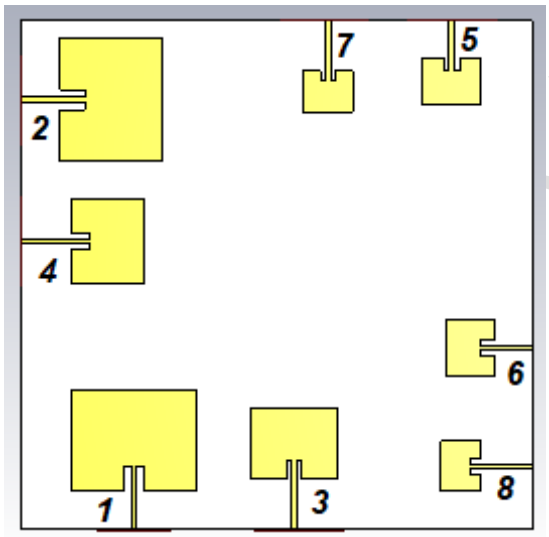

Fig. 4. Proposed dual diversity 8-element MIMO antenna

The premise of the second MIMO antenna design proposed in this study is on the microstrip edge feeding method (without a transformer or notch) and defected ground plane (DGS). The direct coupling of the input signal, as seen in Figure 5, requires a mechanism (DGS was used in this case) to effect patch surface current redistribution and patch size reduction while maintaining a good impedance match between the radiating patch and the feedline [21]. Hence, the initial single-element antenna was designed with a centre frequency of 2.45 GHz and optimized with the aid of CST Studio to match the desired antenna characteristics. The design parameters are given in Table 2. The modelled antennas in CST studio are presented in figures 6 to 8.

Table 2. Design dimensions of single band RMSA with DGS

Design Parameter	Value
Length (L_p)	20.50 mm
Width (W_p)	23.00 mm
Dielectric constant (ε_r)	4.3
Substrate height (h)	1.60 mm
Length of partial ground (Ls)	10.00 mm
Length of substrate (L_g)	35.00 mm
Width of substrate (W_g)	45.00 mm
Width of feedline (W_f)	7.20 mm
Length of ground notch (Lx)	3.20 mm
Width of ground plane notch (Wx)	6.40 mm
Length of 50 Ω transmission line (L_f)	10.00 mm

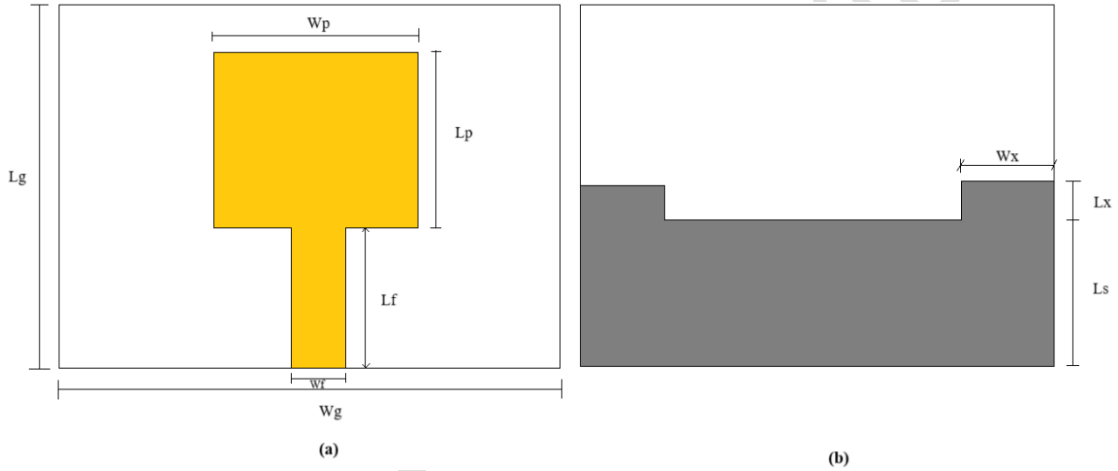

Fig. 5. Proposed single band RMSA with DGS

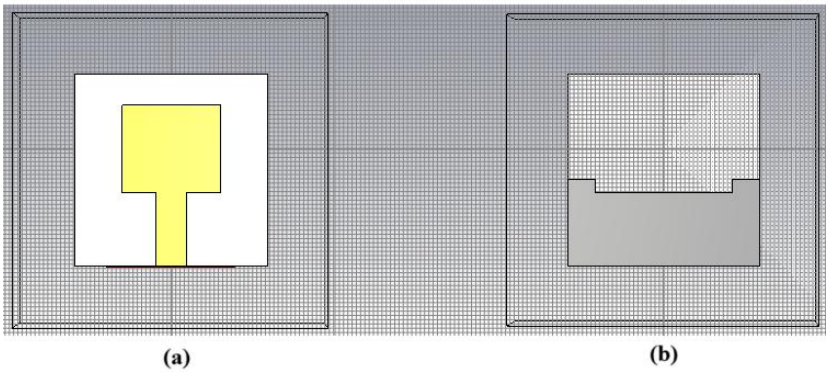

Fig. 6. Modified single-element antenna with DGS (a) top view (b) back view

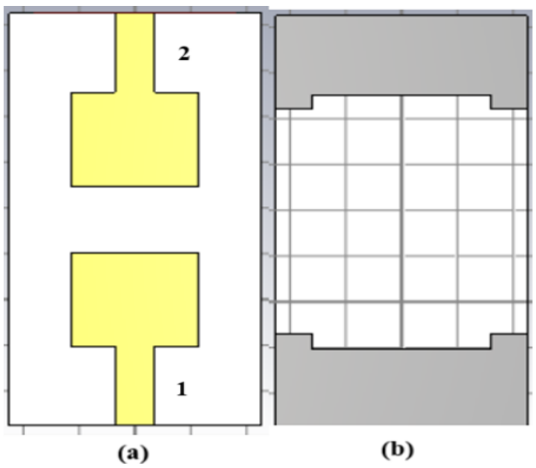

Fig. 7. Proposed 2-element MIMO antenna with DGS (a) top view (b) back view

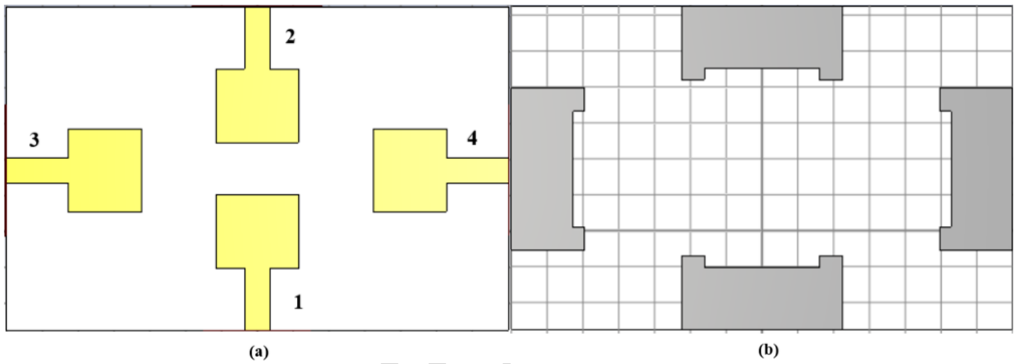

Fig. 8. Proposed 4-element MIMO antenna with DGS (a) top view (b) back view

4. RESULTS AND DISCUSSION

Antenna parameters generally used for antenna analysis, such as s-parameters, gain, and directivity, as well as envelop correlation coefficient (ECC) and diversity gain of the MIMO antennas designed in the previous Section, are presented in this Section.

4.1 S-parameter

The S-parameter achieved by the 8-element antenna at 2.45 GHz (S_{11} and S_{22}), 3.5 GHz (S_{33} and S_{44}), 5.2 GHz (S_{55} and S_{66}) and 6 GHz (S_{77} and S_{88}) are presented in figures 9 to 12. The depicted S-parameters (S_{mn}) designations correspond to typical S_{11} parameter of single-element antenna. Figure 13 gives the combined return loss plot consisting of all antenna elements. Worthy of note, however, is that on all the S-parameter plots presented, a minimum return loss of -36.46 dB was obtained at a centre frequency of 5.2 GHz.

UNDER PEER REVIEW

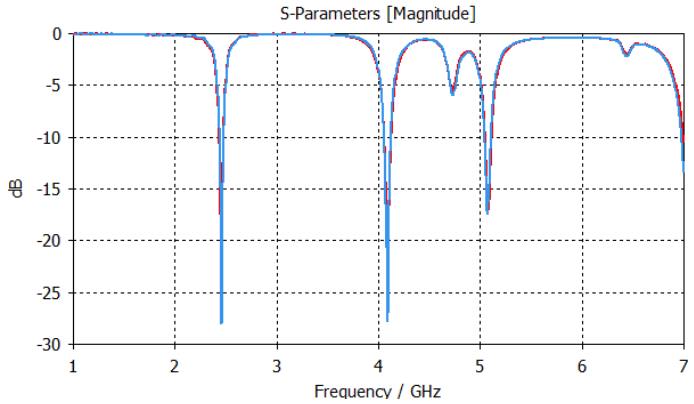

Fig. 9. S-parameter of proposed antenna at 2.45 GHz

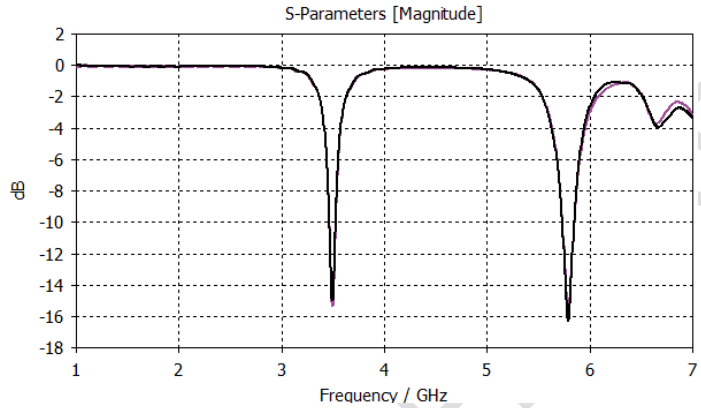

Fig. 10. S-parameter of proposed antenna at 3.5 GHz

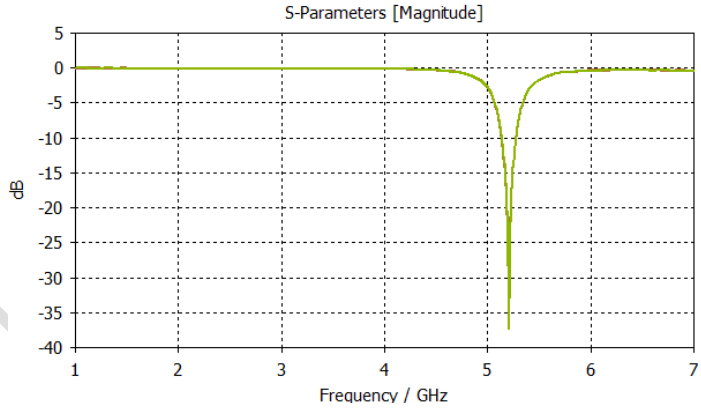

Fig. 11. S-parameter of proposed antenna at 5.2 GHz

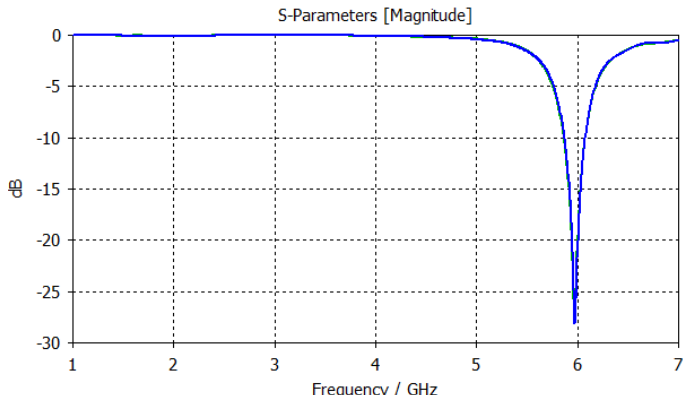

Fig. 12. S-parameter of proposed antenna at 6 GHz

Another notable feature observed from the return loss property illustrated in figure 13 is the somewhat consistent narrow bandwidth recorded at all frequencies of interest. This affirms the lack of a relationship between increased microstrip antenna elements and bandwidth improvement. The dependency of all antenna elements designed at the various centre frequencies on the same substrate was seemingly inconsequential on the return loss values achieved beyond 3.5 GHz.

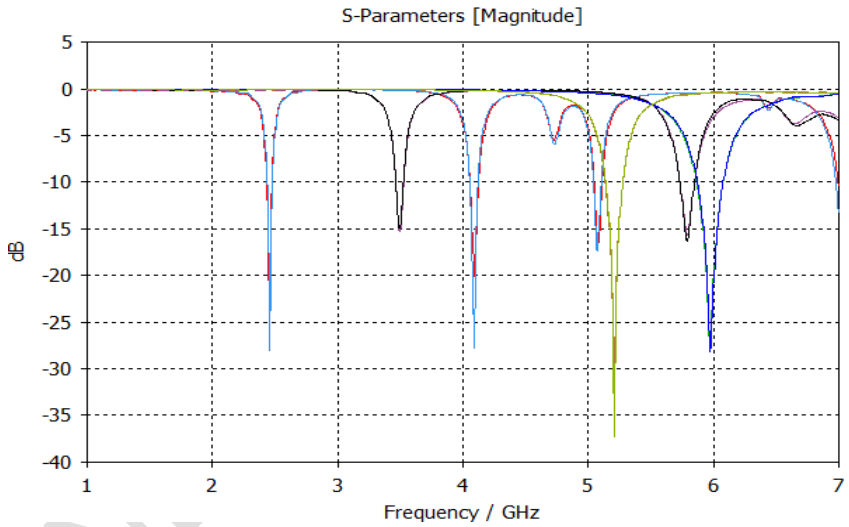

Fig. 13. S-parameter of proposed antenna showing all designed frequencies

The return loss of the single-element microstrip antenna with DGS is presented in Figure 14. An ultrawide bandwidth of 4.8 GHz is evident from the return loss plot in Figure 14, which spans between 2.41 GHz and 7.24 GHz. This implies that the antenna covered most of the UWB, WiMAX, and WiFi bands. A minimum return loss of -45.23 dB was recorded at 5.32 GHz. However, a reduction in bandwidth is noticeable in Figure 15, which illustrates the return loss plot of the 2-element MIMO antenna with DGS.

Further bandwidth reduction is equally seen on the return loss plot of the 4-element MIMO antenna with DGS. By inference, a shift in overall antenna return loss property is observed from the single-element to the 4-element MIMO antenna, reducing bandwidth from 4.8 GHz to 4.22 GHz across design frequencies. Similarly, the minimum return loss value was decreased from -45.23 dB to 25.07 dB. A factor responsible for the notable

shift in antenna property is using the same substrate with independent ground, which leads to surface current redistribution complexities.

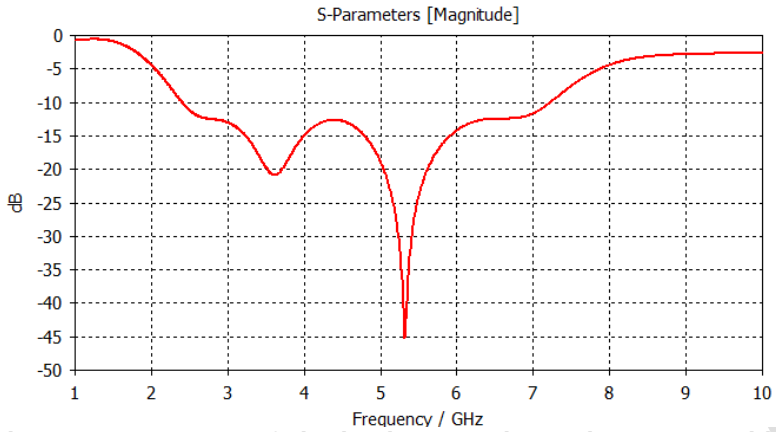

Fig. 14. S-parameter of single-element microstrip antenna with DGS

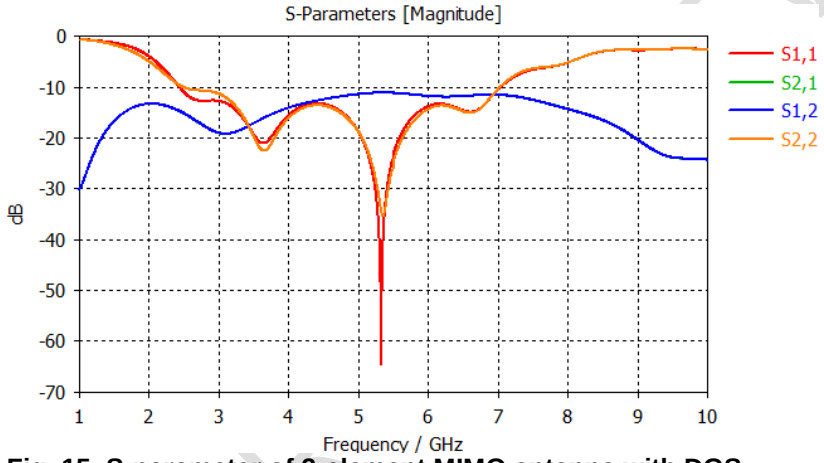

Fig. 15. S-parameter of 2-element MIMO antenna with DGS

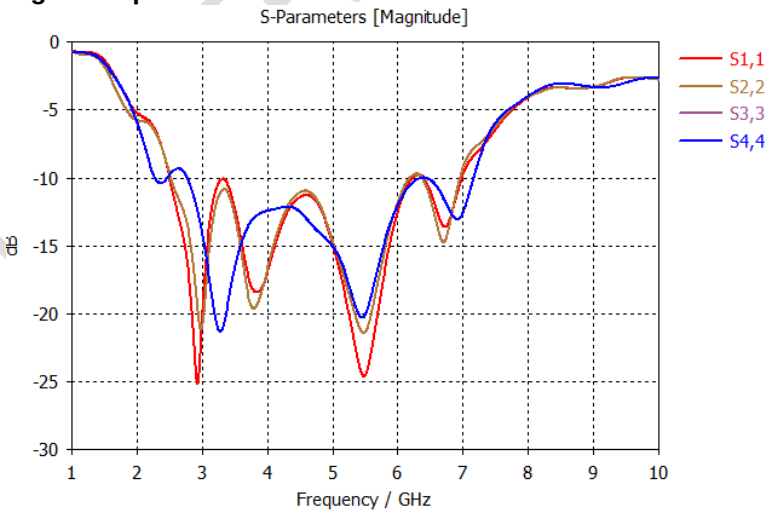

Fig. 16. S-parameter of 4-element MIMO antenna with DGS

4.2 Radiation Pattern and Directivity

The radiation pattern in the E- and H-plane of the 8-element MIMO antenna at 2.45/3.5/5.2/6 GHz is presented in Figures 17 and 18. The H-plane radiation properties are illustrated in Figure 17, in which a nearly omnidirectional pattern was observed at 5.2 GHz. Similarly, the E-plane pattern is presented in Figure 18. A notable characteristic of all the radiation patterns shown is the consistent broadside radiation pattern across the designed frequencies with an average main lobe magnitude of 7.8 dBi.

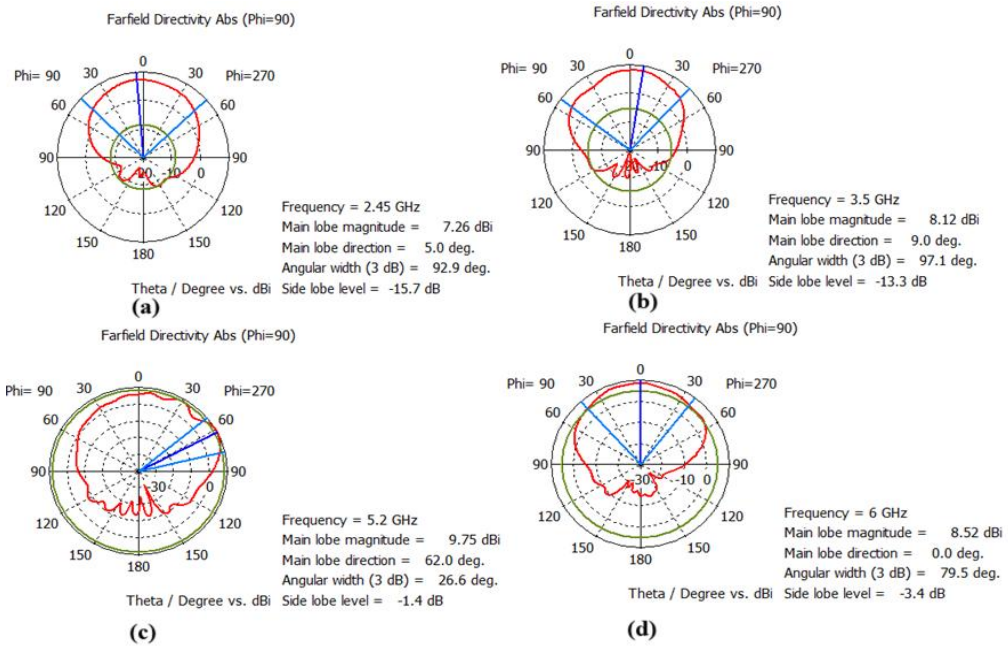

Fig. 17. H-plane of proposed antenna at (a) 2.45 GHz (b) 3.5 GHz (c) 5.2 GHz (d) 6 GHz

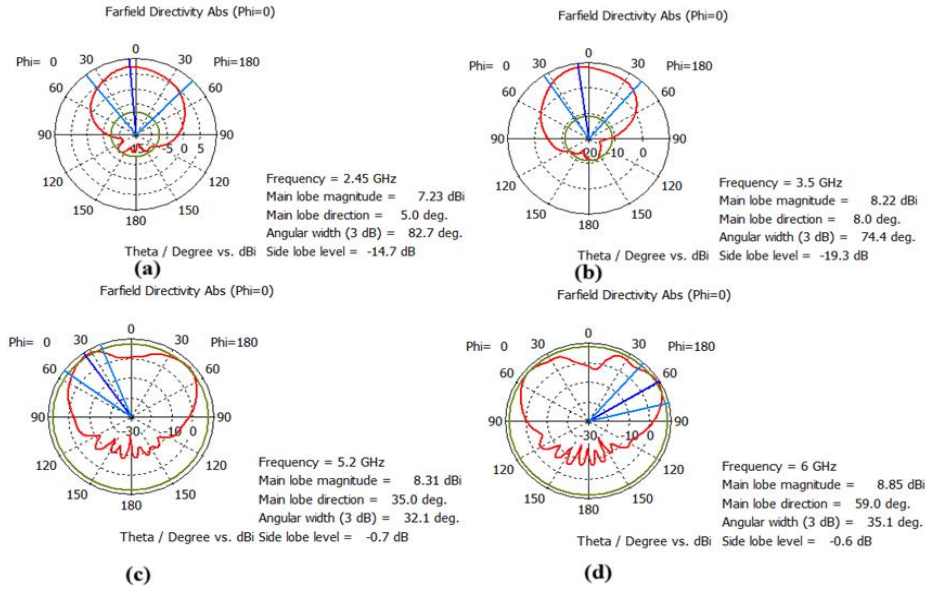

Fig. 18. E-plane of proposed antenna at (a) 2.45 GHz (b) 3.5 GHz (c) 5.2 GHz (d) 6 GHz

Similar to the radiation properties displayed by the 8-element multifrequency MIMO antenna, the 4-element MIMO antenna showed tendencies for omnidirectional radiation patterns across E- and H-plane at the various frequencies of interest, as illustrated in figures 19 to 21. It is worth noting that the plots were extracted from only the first antenna element.

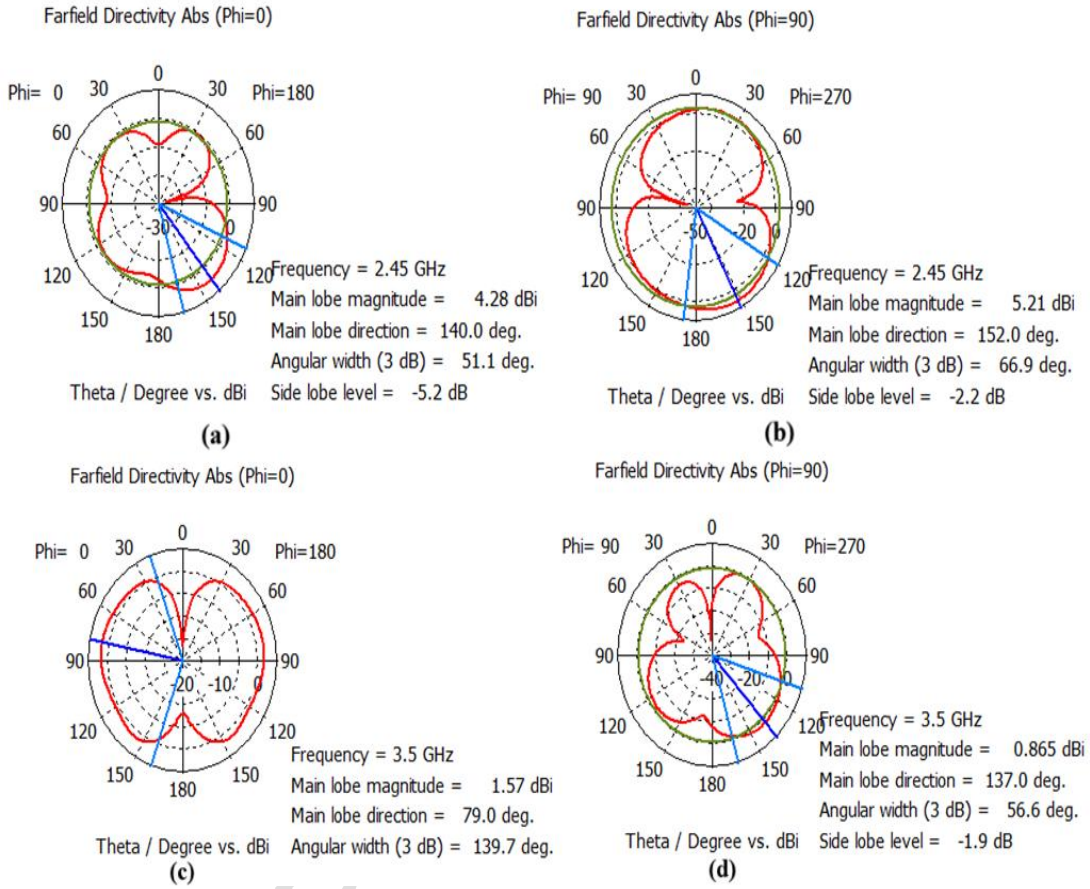

Fig. 19. E- and H-plane of proposed MIMO antenna with DGS at 2.45 and 3.5 GHz

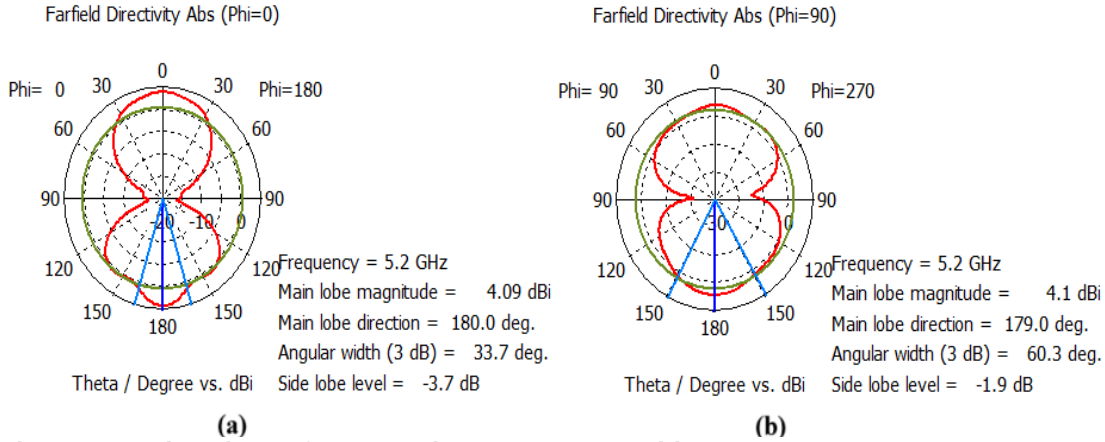

Fig 20. E- and H-plane of proposed MIMO antenna with DGS at 5.2 GHz

4.3 Envelope Correlation Coefficients (ECC) and Diversity Gain (DG)

The Envelope Correlation Coefficients (ECC) and Diversity Gain (DG) of the 8-element multifrequency MIMO antenna are presented in figure 22. At every frequency considered, the proposed antenna averaged ECC and DG values of 8.22×10^{-4} and 9.9999.

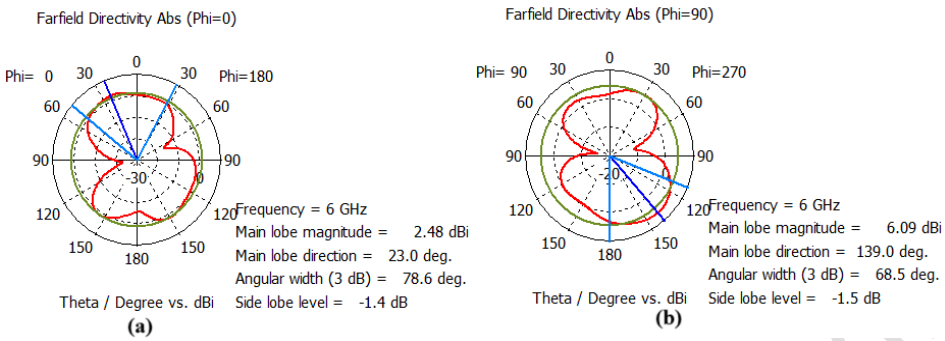

Fig. 21. E- and H-plane of proposed MIMO antenna with DGS at 6 GHz

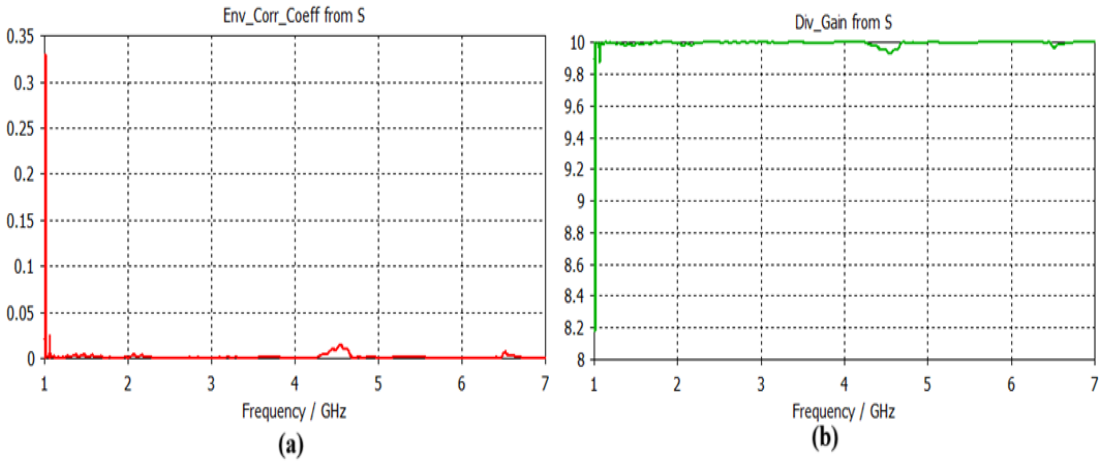

Fig. 22. proposed 8-element MIMO antenna (a) ECC (b) DG

The Envelope Correlation Coefficients (ECC) and Diversity Gain (DG) of the 2- and 4-element MIMO antenna with DGS are presented in figure 23. At every frequency considered, the proposed antenna averaged ECC and DG values of 1.1304×10^{-3} and 9.9943.

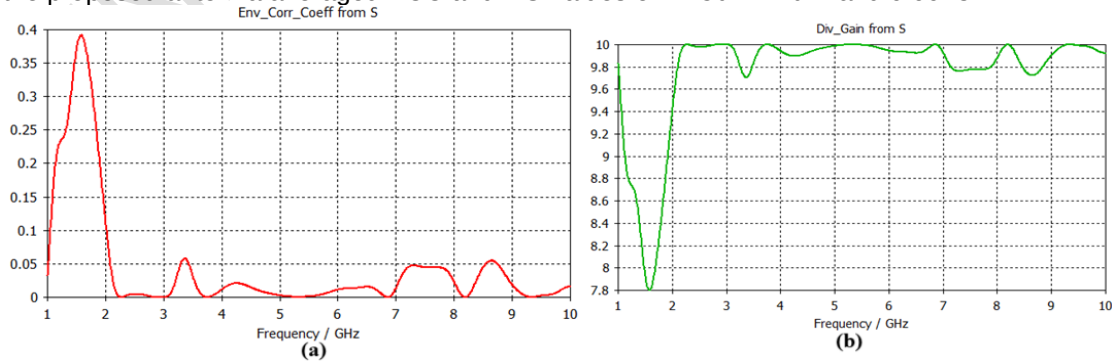

Fig. 23. proposed 4-element MIMO antenna with DGS (a) ECC (b) DG

A brief comparison of ECC and port isolation of the proposed antennas and some selected literature is presented in Table 3.

Table 3.Comparison of ECC and port isolation

Antenna	ECC	Port Isolation
[4]	0.009	13
[5]	0.005	15
[9]	Nil	20
[10]	0.045	15
[20]	0.014	21
2-element MIMO with DGS	0.0014	11
4-element MIMO with DGS	0.0011	14
4-element MIMO	0.0008	33
8-element MIMO	0.000081	27

Also, the antenna gains achieved by the studied antennas were compared with other published works, as presented in Table 4. In comparing the proposed antenna with that presented by [15], it is observed that the antennas proposed achieved comparable antenna gain at higher frequencies of 5.2 and 6 GHz in both the 4-element and 8-element antenna. Also, in terms of size, the antennas proposed by [22], especially the variant with a reflector, occupy a more significant footprint $(220 \times 220 \times 1.6\ mm)$ when compared to the 8-element MIMO antenna $(200 \times 200 \times 1.6\ mm)$ proposed in this study. The 4-element MIMO antenna with DGS has a total footprint of $140 \times 90 \times 1.6\ mm$ which is 26% smaller than the 8-element multifrequency MIMO antenna.

Table 4.Antenna gain comparison

Antenna	Frequency (GHz)	Gain (dB)
[18]	3.3 – 3.8	8.5
[23]	2.2, 3.5, 36	Nil
[24]	29	4.7
[25]	4.5-5.1	3.8
[26]	3.4 - 3.65	4.8
[27]	3.4 – 3.65	2.87
[28]	3.25 – 3.65	3.90
[29]	3.4 – 3.6	2.5
4-element MIMO with DGS	2.45	4.75
	3.50	4.25
	5.20	4.96
	6.00	5.68
4-element MIMO	2.45	6.92
	3.50	6.67
	5.20	7.78
	6.00	7.97
8-element MIMO	2.45	7.26
	3.50	7.43
	5.20	8.23
	6.00	8.58

5. CONCLUSION

In this study, five antennas - 4-element multiband antenna, 8-element multiband dual diversity MIMO antenna, single-element with DGS, 2×1 antenna, and 4-element MIMO

UNDER PEER REVIEW

antenna with DGS – have been designed, simulated, and analyzed; clarifications have been made on several parameters such as return loss, gain, directivity, and radiation pattern as well as ECC and DG for MIMO antennas. From simulation results, a combined bandwidth of 908.68 MHz, average antenna gain of 6.2 dB, and DG of 9.9995 was achieved at all design frequencies considered for the 8-element MIMO antenna. In comparison, the antenna with DGS achieved 4.8 GHz bandwidth as a single-element and 4.22 GHz in multi-element configurations. The frequencies covered by the MIMO antennas studied qualify it for integration in different devices for applications within the designed frequency bands, such as WiMAX, WiFi, and UWB.

UNDER PEER REVIEW

REFERENCES

[1] I. Aldmour, "LTE and WiMAX: Comparison and Future Perspective," Commun. Netw., vol. 05, no. 04, pp. 360–368, 2013, doi: 10.4236/cn.2013.54045.

[2] S. Schwarz, R. W. Heath, and M. Rupp, "Single-user MIMO versus multi-user MIMO in distributed antenna systems with limited feedback," EURASIP J. Adv. Signal Process., vol. 2013, no. 1, p. 54, Mar. 2013, doi: 10.1186/1687-6180-2013-54.

[3] E. Dahlman, P. Stefan, and J. Skold, 4G, LTE-Advanced Pro and The Road to 5G, Third. London, UK: Academic Press, 2016.

[4] H. T. Chattha, "4-Port 2-Element MIMO Antenna for 5G Portable Applications," IEEE Access, vol. 7, no. 4, pp. 96516–96520, 2019, doi: 10.1109/ACCESS.2019.2925351.

[5] M. A. Jamshed, M. Ur-Rehman, J. Frnda, A. A. Althuwayb, A. Nauman, and K. Cengiz, "Dual Band and Dual Diversity Four-Element MIMO Dipole for 5G Handsets," Sensors, pp. 1–13, 2021.

[6] S. Shoaib, I. Shoaib, N. Shoaib, X. Chen, and C. G. Parini, "MIMO Antennas for Mobile Handsets," IEEE Antennas Wirel. Propag. Lett., vol. X, no. c, pp. 1–4, 2015, doi: 10.1109/LAWP.2014.2385593.

[7] S. Nithya, M. Sandhiya, R. Sathish Kumar, S. Vaishnavi, and S. R. Vishnu Prasad, "Design and Fabrication of Microstrip MIMO Antenna for 5G Smart Phones," J. Phys. Conf. Ser., vol. 1916, no. 1, 2021, doi: 10.1088/1742-6596/1916/1/012199.

[8] B. Lee, F. J. Harackiewicz, S. Member, and H. Wi, "Closely Mounted Mobile Handset MIMO Antenna for LTE 13 Band Application," IEEE Antennas Wirel. Propag. Lett., vol. 13, pp. 411–414, 2014.

[9] A. Abdulkareem and M. J. Farhan, "A novel MIMO patch antenna for 5G applications," IOP Conf. Ser. Mater. Sci. Eng., vol. 870, no. 1, 2020, doi: 10.1088/1757-899X/870/1/012040.

[10] S. Singh, A. Kumar Singh, Karunesh, A. Pandey, and R. Singh, "A Novel MIMO Microstrip Patch Antenna for 5G Applications," Proc. - IEEE 2021 Int. Conf. Comput. Commun. Intell. Syst. ICCCIS 2021, pp. 828–833, 2021, doi: 10.1109/ICCCIS51004.2021.9397137.

[11] S. S. Sarade and S. Ruikar, "Development of Multiband MIMO Antenna with Defective Ground Structure: Review," Procedia Comput. Sci., vol. 171, no. 2019, pp. 1829–1838, 2020, doi: 10.1016/j.procs.2020.04.196.

[12] Y. Al-Ajrawi and J. Rahhal, "A simple antenna design for massive MIMO techniques," 2015 JIEEEC 9th Jordanian Int. Electr. Electron. Eng. Conf. JIEEEC 2015, May 2015, doi: 10.1109/JIEEEC.2015.7470743.

[13] E. Sandi, A. Diamah, and M. Al Mawaddah, "High isolation MIMO antenna for 5G C-band application by using combination of dielectric resonator, electromagnetic bandgap, and defected ground structure," Eurasip J. Wirel. Commun. Netw., vol. 2022, no. 1, pp. 1–13, Dec. 2022, doi: 10.1186/S13638-022-02208-1/TABLES/5.

[14] M. A. Al-Tarifi, M. S. Sharawi, and A. Shamim, "Massive MIMO antenna system for 5G base stations with directive ports and switched beamsteering capabilities," IET Microwaves, Antennas Propag., vol. 12, no. 10, pp. 1709–1718, 2018, doi: 10.1049/iet-map.2018.0005.

[15] C. A. Balanis, Antenna Theory, Analysis and Design., 4th ed. New Jersey: John Wiley & Sons, 2016.

[16] Matrix Laboratory, "User's Guide," MATLAB Documentation, 2021.

[17] A. D. Utahile, U. K. Michael, and O. A. Bernard, "Multiband Band and Dual Diversity Eight-Element MIMO Microstrip Antenna for Wireless Applications," J. Eng. Res. Reports, vol. 25, no. 7, pp. 32–42, 2023, doi: 10.9734/jerr/2023/v25i7935.

[18] X. Chen, S. Zhang, and Q. Li, "A Review of Mutual Coupling in MIMO Systems," IEEE Access, vol. 6, pp. 24706–24719, 2018, doi: 10.1109/ACCESS.2018.2830653.

[19] R. Garg, P. Bhartia, I. Bahl, and A. Ittipiboon, Microstrip Antenna Design Handbook. Norwood, MA: Artech House, 2001.

UNDER PEER REVIEW

[20] A. K. Saurabh, P. S. Rathore, and M. K. Meshram, "Compact wideband four-element MIMO antenna with high isolation," Electron. Lett., vol. 56, no. 3, pp. 117–119, 2020, doi: 10.1049/el.2019.2871.

[21] B. Rochani, R. K. Raj, S. Gurjar, and M. Santoshkumar Singh, "Microstrip patch Antenna with defected ground plane for UWB applications," Smart Innov. Syst. Technol., vol. 31, pp. 293–302, 2015, doi: 10.1007/978-81-322-2205-7_28/COVER.

[22] Q. Hua et al., "A Novel Compact Quadruple-Band Indoor Base Station Antenna for 2G/3G/4G/5G Systems," IEEE Access, vol. 7, pp. 151350–151358, 2019, doi: 10.1109/ACCESS.2019.2947778.

[23] N. Agrawal, K. Acharjya, and R. Singh, "5G MIMO Antenna Design with Microstrip Patch Antenna," Int. J. Electron. Commun. Eng., vol. 11, no. 1, pp. 28–38, 2024, doi: 10.14445/23488549/ijece-v11i1p103.

[24] S. Ahmad et al., "A Jug-Shaped CPW-Fed Ultra-Wideband Printed Monopole Antenna for Wireless Communications Networks," Appl. Sci., vol. 12, no. 2, 2022, doi: 10.3390/app12020821.

[25] S. Sharma and M. Kumar, "Design and Analysis of a 4-Port MIMO Microstrip Patch Antenna for 5G Mid Band Applications," Prog. Electromagn. Res. C, vol. 129, no. December 2022, pp. 231–243, 2023, doi: 10.2528/PIERC22120104.

[26] H. S. Abubakar, Z. Zhao, B. Wang, S. H. Kiani, N. O. Parchin, and B. Hakim, "Eight-Port Modified E-Slot MIMO Antenna Array with Enhanced Isolation for 5G Mobile Phone," 2023.

[27] S. H. Kiani et al., "Mimo antenna system for modern 5g handheld devices with healthcare and high rate delivery," Sensors, vol. 21, no. 21, pp. 1–19, 2021, doi: 10.3390/s21217415.

[28] S. H. Kiani et al., "Eight element side edged framed MIMO antenna array for future 5G smart phones," Micromachines, vol. 11, no. 11, pp. 1–13, 2020, doi: 10.3390/mi11110956.

[29] H. Ali et al., "An eight element dual band antenna for future 5g smartphones," Electron., vol. 10, no. 23, pp. 1–12, 2021, doi: 10.3390/electronics10233022.

UNDER PEER REVIEW